3 May 1996

ELSEVIER

Chemical Physics Letters 253 (1996) 333–339

CHEMICAL PHYSICS LETTERS

The UV spectrum of acetyl and the kinetics of the chain reaction between acetaldehyde and chlorine

M. Matti Maricq *, Joseph J. Szente

Research Laboratory, Ford Motor Company, P.O. Box 2053, Drop 3083, Dearborn, MI 48121, USA

Received 13 November 1995; in final form 31 January 1996

Abstract

Time resolved UV spectroscopy has been used to investigate the role of acetyl radical in the photolytically initiated chain reaction of acetaldehyde with chlorine. At a resolution of 2 nm, acetyl has a broad, unstructured, absorption in the 200–280 nm range, with a peak cross section of $(1.07 \pm 0.11) \times 10^{-17}$ cm^2 at 217 nm. The chain propagation reaction between acetyl and molecular chlorine has a measured rate constant of $k_2 = 2.8^{+1.1}_{-0.8} \times 10^{-11}\ e^{(-47 \pm 91)/T}$ cm^3 s^{-1} while the chain terminating self reaction proceeds with a rate constant of $k_3 = 3.9^{+2.3}_{-1.4} \times 10^{-12}\ e^{(450 \pm 120)/T}$ cm^3 s^{-1}.

1. Introduction

Acetyl radicals are important intermediate species in the oxidation of hydrocarbon compounds, whether it be at high temperatures in flames or at low temperatures in the atmosphere. At high temperature the acetyl radical undergoes a competition between dissociation and the addition of molecular oxygen to form acetylperoxy radical. Upon reaction with other hydrocarbons the latter channel leads to the formation of acetyl hydroperoxide, a branching agent that falls apart to give methyl and hydroxyl radicals. Such reactions occurring in the end gas of a cylinder have been implicated in engine knock [1]. At atmospheric temperatures dissociation is too slow to be important, thus the fate of the acetyl radical is conversion to acetylperoxy radical. This compound can react further with NO_2 to form peroxyacetylnitrate, an irritant found in photochemical smog [2].

We are currently investigating the kinetics of a variety of CH_3CO and $CH_3C(O)O_2$ reactions. As other researchers have done, we employ chlorine photodissociation followed by hydrogen abstraction from acetaldehyde to generate the radical species. In the absence of oxygen, the acetyl radical mediates a chain reaction that converts acetaldehyde and molecular chlorine into acetyl chloride and hydrochloric acid. Added oxygen inhibits the chain reaction by competing with chlorine for the acetyl radical. In order to model the kinetics of acetyl and acetylperoxy radicals with other species, accurate rate constants are needed for the reactions involved in their production, providing one impetus for the present study.

The chain reaction of acetaldehyde with chlorine is, however, of interest in its own right. While a

* Corresponding author.

PII S0009-2614(96)00155-8

number of studies of the hydrogen abstraction reaction [3]

$$Cl + CH_3CHO \rightarrow CH_3CO + HCl \quad (1)$$

exist, there is little information about the reaction between acetyl radicals and molecular chlorine

$$CH_3CO + Cl_2 \rightarrow CH_3C(O)Cl + Cl. \quad (2)$$

Under conditions of a high acetaldehyde to chlorine ratio, the major chain termination reaction is the recombination of acetyl radicals,

$$CH_3CO + CH_3CO \rightarrow (CH_3CO)_2 \quad (3)$$

yet considerable discrepancies exist between previous reports of the rate constant for this reaction. The early measurements of Adachi et al. [4] yield a rate constant 2–3 times larger than the subsequent studies by Anastasi and Maw [5], Parkes [6], and Seetula et al. [7], which range from 1.3×10^{-11} to 3.0×10^{-11} $cm^3\ s^{-1}$.

This paper presents new data for the kinetics of reactions (2) and (3) obtained from time resolved UV spectroscopy of the chain reaction between chlorine and acetaldehyde. These results resolve the discrepancies between the previous measurements of k_3. The present study also provides an improved UV spectrum of the acetyl radical, with absolute absorption intensity, that resolves the differences in the previous spectra of Parkes [6] and Adachi et al. [4]. Combining the rate constant k_2 obtained here with the recently reported relative rate [8], k_2/k_4, for the reaction of acetyl with Cl_2 as compared to

$$CH_3CO + O_2 + M \rightarrow CH_3C(O)O_2 + M \quad (4)$$

provides an absolute value of k_4.

2. Experimental

Kinetic measurements of the CH_3CO mediated chain reaction were made using the previously described technique of flash photolysis combined with time resolved UV spectroscopy [9]. A gas mixture of approximately 0.3 Torr of Cl_2 and 3 Torr of CH_3CHO in 100 Torr total pressure of N_2 flows through a fused silica cell 3.2 cm in diameter and 51 cm long. The chain reaction is initiated via Cl_2 photodissociation by directing the 351 nm output from an excimer laser longitudinaly through the cell. A counterpropagating probe beam of broadband UV light from a deuterium lamp is used to monitor the reaction. The light is dispersed by a monochromator and detected by a gated diode array, with the delay between laser pulse and gate varied from 3 to 205 μs. The gate width is 10 μs.

At each time delay the spectrum of the D_2 lamp is recorded immediately prior to the excimer laser pulse as well as at the delay time following the pulse. These measurements of I_0 and I_t, respectively, are converted to absorbances using Beer's law. Wavelength calibration is accomplished by comparison to the spectral lines from a low pressure Hg lamp. Four species contribute to the UV spectrum in the 190–340 nm range: CH_3CO, Cl_2, $CH_3C(O)Cl$, and CH_3CHO, although the last one does so quite weakly. Concentration versus time data is extracted by deconvoluting the absorbance at time t according to the expression

$$\mathrm{Abs}(\lambda, t) = \sum_{i=1}^{4} \sigma_i(\lambda)[i]_t l, \quad (1)$$

where l indicates the path length, $\sigma(\lambda)_i$ is the wavelength dependent UV cross section of species i, and i ranges from 1 to 4 indicating CH_3CO, Cl_2, $CH_3C(O)Cl$, and CH_3CHO, respectively.

Acetaldehyde from Aldrich or Fisher at $> 99\%$ purity is degassed and mixed in a 5 l glass bulb as a 26% mixture with N_2. Chlorine is obtained as a 9.7% mixture in He. The nitrogen buffer gas purity is $> 99.999\%$ with < 1 ppm O_2. This is important because even a small trace of oxygen will quench the chain reaction and make the CH_3CO self reaction appear more rapid than it really is. The acetaldehyde mixture and nitrogen flows are regulated by Tylan flow controllers, whereas the chlorine flow is set by a needle valve. Reproducibility of the Cl_2 flow is checked by measuring the amount of $C_2H_5O_2$ formed when ethane and oxygen replace acetaldehyde and is found to be within 5%. Gas concentrations are established ($\pm 2\%$) by timing the rate of pressure rise from their flow into a fixed volume and are checked for consistency before and after a kinetics run. The gases are precooled/preheated prior to

flowing into the reaction cell, which is kept at various temperature setpoints in the 214–357 K range by a recirculating constant temperature bath. The gas temperature is measured by thermocouples mounted at the inlet and outlet of the reaction cell. At the extreme ends of the range the gas temperature differs from that of the bath fluid by about 10 K.

3. Results

3.1. UV spectrum

Photolysis of a $CH_3CHO/Cl_2/N_2$ gas mixture causes the appearance of a broad, featureless (at 2 nm resolution), almost triangular absorption centered at 217 nm. As Fig. 1 shows, this feature decays on the 100 μs timescale. Concomitantly, a short wavelength feature appears, rising below 200 nm, and a negative absorbance develops in the 270–340 nm region. The latter features are due, respectively, to the formation of acetyl chloride and to the removal of chlorine (and to a much lesser extent acetaldehyde) molecules, as is apparent from a comparison of Fig. 1 to the reference spectra in Fig. 2. The initial absorbance observed at 217 nm is attributed to the acetyl radical.

The CH_3CO spectrum, and its absolute absorption

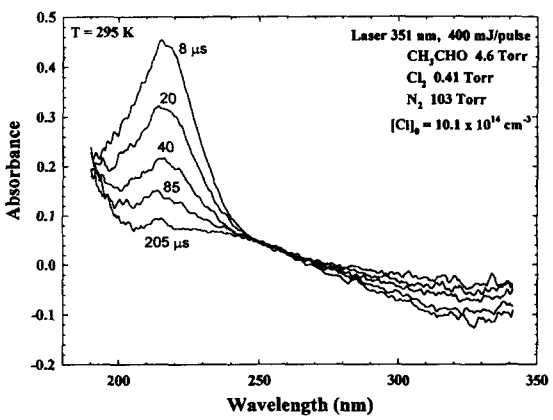

Fig. 1. Time resolved UV spectra of a $CH_3CHO/Cl_2/N_2$ reaction mixture at various delay times following initiation of the chain reaction by excimer laser dissociation of Cl_2. The pulse area is approximately 1 cm^2. Note the negative absorbance in the 280–340 nm region indicating the loss of Cl_2.

Table 1
$CH_3CHO + Cl_2$ chain reaction mechanism

	Reaction	Rate constant
1.	$Cl + CH_3CHO \rightarrow CH_3CO + HCl$	$k = 7.9\times10^{-11}$ cm^3 s^{-1} [11]
2.	$CH_3CO + Cl_2 \rightarrow CH_3C(O)Cl + Cl$	$k = 2.8\times10^{-11}$ $e^{-47/T}$ cm^3 s^{-1} [a]
3.	$CH_3CO + CH_3CO \rightarrow (CH_3CO)_2$	$k = 3.9\times10^{-12}$ $e^{450/T}$ cm^3 s^{-1} [a]
5.	$CH_3CO + Cl \rightarrow$ products	$k = (0-2.4)\times10^{-10}$ cm^3 s^{-1}

[a] Measured in the present study.

intensity, are obtained in the following manner. A spectrum of the $CH_3CHO/Cl_2/N_2$ gas mixture is recorded at early delay times, typically about 3–4 μs after photolysis. Under identical conditions, except that ~ 2 Torr of ethane and ~ 15 Torr of O_2 is substituted for the acetaldehyde, the absorbance of ethylperoxy radicals formed via

$$Cl + C_2H_6 \rightarrow C_2H_5 + HCl$$

$$C_2H_5 + O_2 + M \rightarrow C_2H_5O_2 + M$$

is also recorded. The latter measurement, combined with the known ethylperoxy UV cross section [10], enables a determination of the initial chlorine atom concentration and, thereby, also the initial CH_3CO concentration. Using the reaction model of Table 1, the concentrations of CH_3CO, $CH_3C(O)Cl$, CH_3CHO and Cl_2 present at the 3–4 μs delay time are calculated, enabling small corrections (~ 10%) to be made to the spectrum for the loss of acetyl radicals, the losses of chlorine and acetaldehyde, and the appearance of acetyl chloride. The final result is the spectrum marked CH_3CO in Fig. 2. The error in the assigned cross sections is estimated to be $\pm$10%, with 5% originating from uncertainty in the ethylperoxy cross sections used for concentration calibration and allowing an additional 5% uncertainty for possible small changes in experimental conditions incurred when switching from an acetaldehyde gas mixture to one with ethane and oxygen.

3.2. Kinetics measurements

Application of the deconvolution procedure of Eq. (1) to time resolved spectra, such as those illustrated

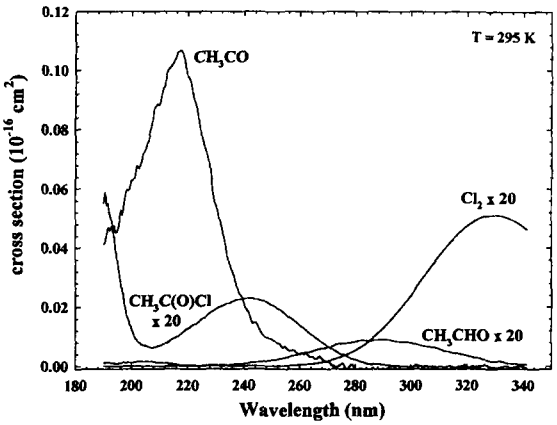

Fig. 2. UV absorption spectra of CH_3CO, $CH_3C(O)Cl$, Cl_2, and CH_3CHO.

in Fig. 1, allows the time dependence of the CH_3CO, $CH_3C(O)Cl$, Cl_2 and CH_3CHO concentrations to be simultaneously ascertained. An example is provided by Fig. 3. Here, an initial acetyl radical population of 6.8×10^{14} cm^{-3} decays over a time span of 200 μs, while at the same time approximately 5×10^{15} cm^{-3} $CH_3C(O)Cl$ molecules are formed and equal numbers of chlorine and acetaldehyde molecules are consumed. The order of magnitude larger changes in acetyl chloride and chlorine concentrations as compared to the initial radical population attest to the existence of a chain mechanism.

Initiation of the chain is provided by photolysis of Cl_2. Chain propagation occurs via reactions (1) and (2). Over short time scales, compared to 100 μs, these reactions establish a steady state ratio of radicals,

$$\frac{[CH_3CO]}{[Cl]} \approx \frac{k_1[CH_3CHO]}{k_2[Cl_2]}$$

which depends on the rate of acetyl formation relative to its removal. When the acetaldehyde concentration is large compared to that of molecular chlorine, the radicals mediating the chain reaction exist primarily in the CH_3CO state; in contrast a low $[CH_3CHO]$ to $[Cl_2]$ ratio implies that the radical population is dominated by chlorine atoms.

As can be deduced from the conditions reported in Table 2, the present experiments were performed under conditions supporting a high $[CH_3CO]/[Cl]$ ratio (results from two experiments employing a ratio near unity are provided for comparison). Thus, the principal chain termination step is reaction (3), the recombination of acetyl radicals. The reaction between chlorine atoms and acetyl radicals,

$$Cl + CH_3CO \rightarrow CH_2CO + Cl \quad (5)$$

could also play a role because, in spite of conditions ensuring a small chlorine atom concentration, it is possible that this reaction has a large rate constant.

Table 2
Measured rate constants

Temp (K)	Conditions				Results	
	CH_3CHO (Torr)	Cl_2 (Torr)	P_{tot} (Torr)	$[Cl]_0$ (10^{14} cm^{-3})	k_2 (10^{-11} cm^3 s^{-1})	k_3 (10^{-11} cm^3 s^{-1})
214	2.1	0.22	96	7.2	2.1 ± 0.5	3.0 ± 0.9
234	2.4	0.22	99	6.6	2.4 ± 0.8	3.4 ± 1.5
235	2.3	0.22	98	7.0	2.4 ± 0.5	2.6 ± 0.8
254	2.7	0.22	102	6.8	2.5 ± 0.4	2.1 ± 0.4
256 [a]	0.89	0.53	107	6.7	1.8 ± 0.4	2.7 ± 1.7
274	2.9	0.25	99	6.8	2.2 ± 0.4	2.2 ± 0.4
294	3.0	0.22	105	6.1	2.7 ± 0.5	1.7 ± 0.4
295 [a]	0.74	0.43	104	5.1	2.7 ± 0.5	1.6 ± 1.7
295	4.6	0.41	108	10.1	2.2 ± 0.4	1.7 ± 0.4
325	2.9	0.24	103	7.1	2.4 ± 0.4	1.6 ± 0.3
357	3.1	0.25	107	6.2	2.4 ± 0.5	1.5 ± 0.3

[a] Experiments were carried out with moderate as opposed to high $[CH_3CHO]/[Cl_2]$ ratio and the rate constants fit with $k_5 = (1.2 \pm 1.2) \times 10^{-10}$ cm^3 s^{-1}. Note the resulting large error bars in k_3. These rate constant data are not included in the fits of k_2 or k_3 to their Arrhenius expressions.

For comparison, the $Cl + C_2H_5 \rightarrow C_2H_4 + HCl$ reaction has a rate constant of 2.9×10^{-10} cm^3 s^{-1} [11]. With both the small steady state chlorine atom concentration and the slow rate of chlorine atom recombination, the termination reaction

$$Cl + Cl + M \rightarrow Cl_2 + M$$

plays a negligible role in the present experiments.

Rate constants for reactions (2) and (3) are extracted from the concentration versus time profiles by fitting to the data the reaction model in Table 1. The initial radical concentration is measured independently by substituting ethane and oxygen for acetaldehyde, as described in Section 3.1. k_2 and k_3 are varied to obtain simultaneously the minimum squared deviations between the data and the model predictions for 20[CH_3CO], [$CH_3C(O)Cl$], and the changes in [Cl_2] and $\frac{1}{2}$[CH_3CHO]. The factor of 20 weighting for the acetyl radical concentration is due to the roughly factor of 20 increase in sensitivity of the UV spectrometer for CH_3CO as opposed to the other two species (see Fig. 2). Similar reasoning applies to the acetaldehyde weighting. The best fits are illustrated by the solid lines in Fig. 3. The reader may notice a systematic underprediction of [$CH_3C(O)Cl$] and an overprediction of Δ[Cl_2]. This likely occurs because of a systematic discrepancy between the reference spectra of the four species that are fit. The discrepancies, however have a negligible effect on k_2 and k_3. For example, [$CH_3C(O)Cl$] and Δ[Cl_2] are much better fit if acetaldehyde is omitted from the deconvolution procedure of Eq. (1); yet the effect on k_2 and k_3 is within their respective error bars.

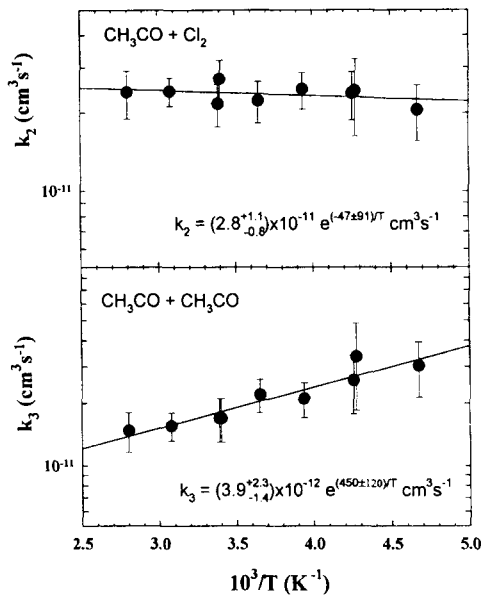

Fig. 4. Top: Temperature dependence of the rate constant for the $CH_3CO + Cl_2$ reaction; bottom: temperature dependence of the rate constant for the CH_3CO self reaction.

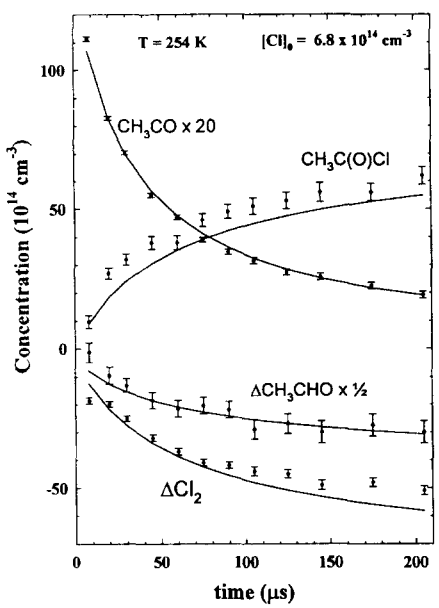

Fig. 3. Concentration versus time profiles for [CH_3CO], [$CH_3C(O)Cl$], and the changes in [Cl_2] and [CH_3CHO], as determined by least-squares fits of time resolved spectra, such as those in Fig. 1, to linear superpositions of the reference spectra in Fig. 2. The best-fit rate constants are $k_2 = (2.5 \pm 0.4) \times 10^{-11}$ cm^3 s^{-1} and $k_3 = (2.1 \pm 0.4) \times 10^{-11}$ cm^3 s^{-1}.

The rate constants determined from the above fitting procedure are listed in Table 2 and illustrated versus $1000/T$ in Fig. 4. Upon comparison to the Arrhenius expression, the reaction of acetyl with molecular chlorine has a very nearly temperature independent rate constant of $k_2 = 2.8^{+1.1}_{-0.8} \times 10^{-11}$ $e^{(-47 \pm 91)/T}$ cm^3 s^{-1}. The self reaction of CH_3CO exhibits a small negative temperature dependence with $k_3 = 3.9^{+2.3}_{-1.4} \times 10^{-12}$ $e^{(450 \pm 120)/T}$ cm^3 s^{-1}.

Contributions to the errors in k_2 and k_3 come

from a variety of sources, such as uncertainties in the UV cross sections of the species that are monitored, uncertainties in the concentrations of CH_3CHO and Cl_2, and the uncertainty in k_1. On the other hand, the successful fitting of all four concentration profiles supports the accuracy of the reaction model and lends confidence to the rate constants that are derived. Noise in the concentration versus time data contributes a 5%–10% error to k_2. The uncertainties of 10% in σ_{CH3CO} and 5% each in $\sigma_{CH3C(O)Cl}$ and σ_{Cl2} transfer to the same fractional errors in k_2. A 5% uncertainty in $[Cl_2]$ leads to a 14% error in the rate constant. In contrast, an uncertainty of 5% in $[CH_3CHO]$, variation of k_1 by 10%, or k_5 by $\pm 1 \times 10^{-10}$ cm^3 s^{-1} and the uncertainty in σ_{CH3CHO} have only small effects on the determination of k_2. Combining these errors in a statistically independent manner produces an overall error of approximately $\pm 20\%$.

As might be anticipated from the radical–radical nature of reaction (3), it is relatively insensitive to the uncertainties in $\sigma_{CH3C(O)Cl}$ and σ_{Cl2} and to the initial chlorine and acetaldehyde concentrations. The largest source of error is the 10% uncertainty in σ_{CH3CO}, which contributes an approximately 20% error to k_3. Noise introduces another 5%–10% error, whereas the contribution from varying k_5 between $(0–2.4) \times 10^{-10}$ cm^3 s^{-1} ranges from 8%–15%, increasing with increasing initial radical concentration. The overall error in k_3 is estimated at $\pm 25\%$. As evident from the two experiments in Table 2 with $[CH_3CHO]/[Cl_2] \approx 1$, the sensitivity of k_3 to reaction (5) increases substantially as this ratio decreases.

4. Discussion

The shape of the CH_3CO spectrum obtained in the present work, and exhibited in Fig. 2, agrees well with the spectrum reported by Parkes [6]. Both show a steep rise in intensity beginning at 240 nm; however, the maximum of the present spectrum occurs at 217 nm, at about 5 nm longer wavelength than that of Parkes. Also, we observe a shoulder rising from 280–240 nm, possibly due to a second electronic transition. A comparison of the absorption intensities cannot be made because Parkes was unable to measure the photolysis rate in his experiments. In contrast, the present spectrum differs considerably from that of Adachi et al. [4] The latter authors show a spectrum with two maxima, whereas we observe only one; however, they report observing only a single peak for CD_3CO. Subsequently, Basco and Parmar [12] remeasured the CH_3CO spectrum, showing it to have a single maximum at 216 nm in agreement with the present spectrum. However, the peak absorption cross section of 1.7×10^{-17} cm^2 recorded by Adachi et al. [4], and adopted by Basco and Parmar [12], is about 50% larger than our value of 1.07×10^{-17} cm^2. It is possible that the discrepancy originates because of the much larger value of k_3 that Adachi et al. [4] used to extrapolate the absolute intensity from spectra recorded 48 to 156 μs after photolysis.

To our knowledge there are no previously reported measurements of the rate constant for the reaction of acetyl radical with molecular chlorine with which to compare our results. The very small positive temperature dependence implies a nearly barrierless reaction. This is consistent with the small activation energies found for other hydrocarbon radical reactions with Cl_2, such as 0 K for HCO, 361 K for CH_3 and 0 K for t-C_4H_9 [13]. If we combine our value of k_2 with the relative rate $k_2/k_4 = 7.9$ reported by Kaiser and Wallington [8], we obtain a rate constant of $k_4 = 3.1 \times 10^{-12}$ cm^3 s^{-1} at 295 K for the addition of O_2 to the acetyl radical. This value is typical of the rate constants for hydrocarbon radical – O_2 addition reactions [3].

Previous reports of the CH_3CO self reaction rate constant have varied widely. Adachi and co-workers [4] first found the very high rate constant of 7.5×10^{-11} cm^3 s^{-1} at 295 K and later the somewhat smaller value of 5.8×10^{-11} cm^3 s^{-1}. The group of Kalliorinne, Koskikallio, and co-workers [7,14,15] have reported rate constants ranging from 1.8×10^{-11} cm^3 s^{-1} to 4.0×10^{-11} cm^3 s^{-1}. Consistent with the smaller value, Parkes [6] derived a rate constant of 3.0×10^{-11} cm^3 s^{-1} for the self reaction. Anastasi and Maw [5] studied the reaction as a function of temperature and found the rate constant to decrease slightly from 1.3×10^{-11} cm^3 s^{-1} at 263–303 K to 1.1×10^{-11} cm^3 s^{-1} at 343 K. The present experiments explore the acetyl radical self reaction over a larger temperature range. They yield rate constants decreasing gradually from 3.0×10^{-11}

$cm^3\ s^{-1}$ at 214 K to $1.5 \times 10^{-11}\ cm^3\ s^{-1}$ at 357 K. The room temperature value of $2.4 \times 10^{-11}\ cm^3\ s^{-1}$ is considerably smaller than the values of Adachi et al. [4], Timonen et al. [15], and Parkes [6]. It agrees well with Seetula et al. [7] and is about 50% larger than the value of Anastasi and Maw [5]. Many of the previous experiments relied on the photolysis of various ketones, such as acetone, to generate the acetyl radical; however, in the process they also produced other radicals, for example, methyl. Competing reactions by these radicals could well increase the apparent CH_3CO self reaction rate. In contrast, Anastasi and Maw [5] used the photolysis of azomethane followed by the addition of CO to CH_3 to generate the acetyl radical. The slow rate of the addition step could account for an underestimate of the CH_3CO self reaction rate constant.

5. Conclusion

Photolysis of Cl_2 in the presence of acetaldehyde initiates an efficient chain reaction. The study of this chain by time resolved UV spectroscopy provides a means by which to measure the rate constant for the propagation step of acetyl radical reacting with molecular chlorine. This reaction is found to be both fast and essentially independent of temperature. By adjusting the acetaldehyde to Cl_2 concentration ratio to be high, the steady state radical population is driven to consist predominantly of acetyl radicals. Under such conditions, the acetyl radical self reaction dominates chain termination and enables the measurement of its rate constant. The self reaction rate constant is relatively fast and exhibits a small negative temperature dependence.

References

[1] E. W. Kaiser, C. K. Westbrook and W. J. Pitz, Intern. J. Chem. Kinetics 18 (1986) 655.
[2] R. P. Wayne, Chemistry of Atmospheres, (Clarendon, Oxford, 1991).
[3] W. G. Mallard, F. Westley, J. T. Herron, R. F. Hampson and D. H. Frizzell, NIST Chemical Kinetics Database: Version 6.0, (NIST, Gaithersburg, 1994).
[4] H. Adachi, N. Basco and D. G. L. James, Chem. Phys. Letters 59 (1978) 502; Intern. J. Chem. Kinet. 13 (1981) 1251.
[5] C. Anastasi and P. R. Maw, J. Chem. Soc. Faraday Trans. I 78 (1982) 2423
[6] D. A. Parkes, Chem. Phys. Letters 77 (1981) 527.
[7] J. Seetula, K. Blomquist, K. Kalliorinne and J. Koskikallio, Acta Chem. Scandinavica 40 (1986) 658; Finn. Chem. Letters 61 (1985) 139.
[8] E. W. Kaiser and T. J. Wallington, J. Phys. Chem. 99 (1995) 8669.
[9] M. M. Maricq and J. J. Szente, J. Phys. Chem. 96 (1992) 10862.
[10] M. M. Maricq and T. J. Wallington, J. Phys. Chem. 96 (1992) 986.
[11] M. M. Maricq, J. J. Szente and E. W. Kaiser, J. Phys. Chem. 97 (1993) 7970.
[12] N. Basco and S. S. Parmar, Intern. J. Chem. Kinet. 17 (1985) 891.
[13] J. A. Seetula, D. Gutman, P. D. Lightfoot, M. T. Rayes and S. M. Senkan, J. Phys. Chem. 95 (1991) 10688.
[14] E. Hassinen, K. Kalliorinne and J. Koskikallio, Intern. J. Chem. Kinetics 22 (1990) 741.
[15] R. Timonen, K. Kalliorinne, K. Blomquist and J. Koskikallio, Int. J. Chem. Kinetics 14 (1982) 35.